Soliton concepts and the protein structure

Andrei Krokhotin,[1, *] Antti J. Niemi,[2, 1, †] and Xubiao Peng[1, ‡]

[1]*Department of Physics and Astronomy, Uppsala University, P.O. Box 803, S-75108, Uppsala, Sweden*
[2]*Laboratoire de Mathematiques et Physique Theorique CNRS UMR 6083,*
Fédération Denis Poisson, Université de Tours, Parc de Grandmont, F37200, Tours, France

Structural classification shows that the number of different protein folds is surprisingly small. It also appears that proteins are built in a modular fashion, from a relatively small number of components. Here we propose to identify the modular building blocks of proteins with the dark soliton solution of a generalized discrete nonlinear Schrödinger equation. For this we show that practically all protein loops can be obtained simply by scaling the size and by joining together a number of copies of the soliton, one after another. The soliton has only two loop specific parameters and we identify their possible values in Protein Data Bank. We show that with a collection of 200 sets of parameters, each determining a soliton profile that describes a different short loop, we cover over 90 % of all proteins with experimental accuracy. We also present two examples that describe how the loop library can be employed both to model and to analyze the structure of folded proteins.

I. INTRODUCTION

Proteins come in many shapes, but the number of different folds is definitely much smaller than suggested by Levinthal's estimate [1]. For example, thus far the structural classification scheme SCOP [2] has identified 1393 unique folds while in CATH [3] here are currently 1282 topologies. These figures have not changed since the year 2008, indicating that the number of different protein conformations is quite limited and probably most of them have already been observed. Furthermore, the great success of SCOP, CATH and other approaches such as FSSP [4] in classifying the architecture of proteins is a manifestation that proteins are built in a modular fashion from a relatively small number of different components.

Here we advocate a quantitative energy function based approach to identify and classify the modular components of proteins. We propose to utilize the dark soliton solution of a generalized discrete nonlinear Schrödinger (DNLS) equation as the basic modular building block. The original DNLS equation [6], [7] shares a long history with protein research. The equation was introduced by Davidov to explain how an energy excitation propagates along the α-helix [8], [9]. The soliton evokes a deformation of the protein shape, and as a consequence a trapped soliton is a natural cause for protein folding. The present generalization of the original DNLS equation is motivated by recent observations that protein loops in the HP35 villin headpiece with Protein Data Bank (PDB) [10] code 1YRF [11], and in the myoglobin with PDB code 1ABS [12] are accurately described in terms of its dark soliton. In this article we extend this observation to essentially all proteins in PDB. We propose to classify the shapes of loops in terms of a small number of universal parameters that appear in the generalized DNLS

equation. These parameters specify the global characteristics such as the size and location of a short loop that is described by a single soliton. But the detailed shape of this loop is entirely determined by the soliton solution. Each set of the soliton parameters then corresponds to a different short fundamental loop and these fundamental loops constitute the modular building blocks of proteins.

We adopt the present experimental precision as the quantitative criterion for identifying two different protein structures. The accuracy of x-ray measurements which is the dominant approach to structure determination, is measured by the B-factor. For very high resolution structures the backbone C_α carbons have B-factor values that are typically less than [13]

$$B_{max} \overset{<}{\sim} 35 \text{ Å}^2 \qquad (1)$$

According to the Debye-Waller relation this corresponds to a fluctuation distance that is less than or equal to

$$\sqrt{<x^2>}_{max} = \sqrt{\frac{B_{max}}{8\pi^2}} \approx 0.65 \text{ Å} \qquad (2)$$

Consequently we identify two structures if they deviate from each other no more than $0.6 - 0.7$ Å in RMSD. Indeed, when the RMSD value between two loop configurations is less than this cut-off value, present experimental techniques can not reliably differentiate between them so that for all practical purposes the two structures are identical. Here we show that it is sufficient to introduce only 200 distinct parameter sets for the soliton, constructed using 44 different proteins, in order to describe over 90% of known protein structures with the B-factor accuracy. Consequently the number of different modular protein components appears to be almost an order of magnitude smaller than suggested by the present SCOP and CATH data. Since the purpose here is to show that we have a method that works, we do not aim to optimize the loop library. But we suspect that the actual number of truly independent loops is much smaller, probably less than 100. For this we show that the 200 fundamental loops can be described by 57 multiple covered loops.

---

*Electronic address: Andrei.Krokhotine@cern.ch
†Electronic address: Antti.Niemi@physics.uu.se
‡Electronic address: xubiaopeng@gmail.com

II. MODEL

We characterize the shape of a protein in terms of its central C_α backbone. These carbon atoms are located at the positions $\mathbf{r}_i$ where $i = 1, ..., N$ label the residues. For each pair of nearest neighbors $\mathbf{r}_{i+1}$ and $\mathbf{r}_i$ we introduce the unit tangent vector and the unit bi-normal vector, respectively

$$\mathbf{t}_i = \frac{\mathbf{r}_{i+1} - \mathbf{r}_i}{|\mathbf{r}_{i+1} - \mathbf{r}_i|} \qquad \& \qquad \mathbf{b}_i = \frac{\mathbf{t}_{i-1} \times \mathbf{t}_i}{|\mathbf{t}_{i-1} \times \mathbf{t}_i|} \quad (3)$$

Then

$$\psi_i = \arccos(\mathbf{t}_{i+1} \cdot \mathbf{t}_i) \quad \& \quad \theta_i = \arccos(\mathbf{b}_{i+1} \cdot \mathbf{b}_i) \quad (4)$$

are the standard discrete Frenet frame bond angle and torsion angle of the backbone. Note that the bond angle ψ_i is determined by three C_α carbons, those at the sites $\mathbf{r}_i$, $\mathbf{r}_{i+1}$ and $\mathbf{r}_{i+2}$. But for the torsion angle θ_i we need four C_α carbons, those between sites $i - 1$ and $i + 2$. Inversely if the bond and torsion angles are known we can reconstruct the entire protein backbone by solving the discrete Frenet equation. We refer to [14] for details of the present coordinate system.

An excellent approximation to the standard right-handed α-helix and the β-strand is obtained by setting

$$(\psi_i, \theta_i)_\alpha \approx (\frac{\pi}{2}, 1) \quad \& \quad (\psi_i, \theta_i)_\beta \approx (1, \pi) \quad (5)$$

Similarly, we get the other familiar regular secondary structures like 3/10 helices, left-handed helices *etc.* by selecting proper constant values for the bond and torsion angles. We also record that the following $\mathbb{Z}_2$ transformation leaves the backbone coordinates intact [14]

$$\begin{aligned} \psi_k &\to -\psi_k \qquad \text{for all} \quad k \geq i \\ \theta_i &\to \theta_i - \pi \end{aligned} \quad (6)$$

Loops are configurations that bridge between these regular secondary structures. Elsewhere [11], [12] it has been shown that loops in the chicken villin headpiece with PDB code 1YRF and the myoglobin 1ABS can be described in terms of the dark soliton of the generalized discrete nonlinear Schrödinger equation that derives from the energy function

$$E = -\sum_{i=1}^{N-1} 2\,\psi_{i+1}\psi_i$$

$$+\sum_{i=1}^{N}\left\{ 2\psi_i^2 + q \cdot (\psi_i^2 - \mu^2)^2 + \frac{r}{2} \cdot \psi_i^2 \theta_i^2 - v \cdot \theta_i + \frac{w}{2} \cdot \theta_i^2 \right\} \quad (7)$$

where (q, μ, r, v, w) are parameters. Here the first sum together with the three first terms in the second sum comprise exactly the energy of the standard DNLS equation [11]. The fourth (v) is a conserved quantity in the

DNLS hierarchy [7], called the "helicity". We note that the conserved "momentum" could also be added [7] but since the improvement in accuracy is minor we leave it out. The last (w) is the Proca mass term that we include for completeness. In this manner the functional form (7) becomes deeply anchored in the elegant mathematical structure of integrable hierarchies [7]. But unlike *e.g.* force fields in molecular dynamics, the energy function (7) does not purport to explain the fine details of the atomary level mechanisms that give rise to protein folding. Instead, in line with Landau-Lifschitz theories it describes the properties of a folded protein backbone in terms of universal physical arguments.

In [11] it has been shown that (7) supports solitons. For this we first eliminate the variable θ_i in terms of ψ_i,

$$\theta_i[\psi_i] = \frac{v}{w + r\,\psi_i^2} \equiv \frac{b}{1 + e\,\psi_i^2} \quad (8)$$

If the value of θ_i falls outside of its fundamental domain $[-\pi, \pi]$ we redefine it modulo 2π.

We vary the energy function with respect to ψ_i and substitute $\theta_i[\psi_i]$ from (8) to arrive at

$$\psi_{i+1} - 2\psi_i + \psi_{i-1} = U'[\psi_i]\psi_i \equiv \frac{dU[\psi]}{d\psi_i^2}\,\psi_i \quad (i = 1, ..., N) \quad (9)$$

with $\psi_0 = \psi_{N+1} = 0$. This is a generalization of the DNLS equation with

$$U[\psi] = -\frac{1}{2}v \cdot \theta[\psi] - 2q\mu^2 \cdot \psi^2 + q \cdot \psi^4$$

$$= -(2q\mu^2 - \frac{1}{2}vbe)\psi^2 + (q - \frac{1}{2}vbe^2)\psi^4 + ... \quad (10)$$

where we recognize the familiar structure of the nonlinear Schrödinger equation potential [6]-[9]. Indeed, it turns out that in the case of proteins the correction terms give rise to an adjustment that is tiny in comparison to the B-factor accuracy.

The exact dark soliton solution to the discrete nonlinear Schrödinger equation is not known in a closed form. But it should be a discrete version of the continuum solution, and thus an excellent approximation is obtained by *naive* discretization of the continuum dark NLSE soliton [6]-[9]:

$$\psi_i = \frac{(m_1 + 2\pi N_1) \cdot e^{c_1(i-s)} - (m_2 + 2\pi N_2) \cdot e^{-c_2(i-s)}}{e^{c_1(i-s)} + e^{-c_2(i-s)}} \quad (11)$$

Here s is a parameter that determines the backbone site location of the center of the fundamental loop that is described by the soliton. The $m_{1,2} \in [0, \pi]$ are parameters that in the continuum limit coincide known combinations of the parameters in (10) [6]-[9]; in the case of proteins their values are entirely determined by the adjacent helices and strands. The N_1 and N_2 constitute the integer parts of $m_{1,2}$, initially we take $N_1 = N_2 \equiv N$. This integer is like a covering number, it determines how many

TABLE II: The sites of the loop structures (11), (8) that we identify in 1A6M. Indexing starts from the N terminus. We also display the number of matches we have in our data set when we use as a cut-off value 0.5 Å in RMSD distance.

Sites	1Matches
8-23	525
34-39	702
41-46	610
48-54	183
56-61	819
77-83	2
81-87	1501
95-100	298
96-100	2352
122-127	287

to eliminate one of these two loops. However, this would be highly questionable as it would also push us below the experimental B-factor accuracy and that does not make much sense. We adopt the position that 0.5 Å is about the best one can do in identifying the fundamental loops, with presently available experimental data.

We continue by selecting a new protein structure. We perform the same visual identification of loops. We continue the process until we have identified a total of exactly 200 loops such that *each pair* of these loops, with the same number of sites, has a mutual RMSD distance that exceeds 0.5 Å. For this we only need to go thru 44 randomly chosen protein structures in our data set, the proteins are listed in Table III.

1A6M(A)	2OVG(A)	2O7A(A)	1XG(D)	1LWB(A)
1SAU(A)	2I4A(A)	3GOE	2AIB	1P6O
2VZC(A)	1WMA(A)	3F1L(B)	1MUN(A)	3PD7(B)
1WKQ(B)	3E7R(L)	3OQ2(A)	3BFQ(G)	1SEN(A)
1MN8(C)	3CT6(A)	2XL6(A)	3A5F(B)	3CI3(A)
3G46(A)	1ZZK(A)	1PSR(A)	1I27(A)	1P1X(B)
2V9V(A)	2W72(A)	1OAI(A)	3DNJ(A)	1NNF(A)
3LB2(A)	1Q6O(B)	3P3C(A)	1QNR(A)	3L0F(A)
1DO4(A)	3OGN(B)	3MBX(B)	2W91(A)	-

TABLE III: The PDB codes of the 44 proteins that we have used in constructing our loop library (with chain in parentheses)

These 200 loop structures have between 5 and 9 sites, including the two end points that are in regular secondary structure positions. The distribution of the number of loops according to their size is shown in Table IV.

Loops with length 6 are by far the most common and we only identify seven length 8 loops, only one fundamental loop with length 9, and none longer. We suspect that the very few length 8 loops and the single length 9 loop can probably be interpreted as combinations of length 5 and 6 loops by an extended search of fundamental loops; The purpose of the present article is not to develop a publicly available databank but to form a conceptual basis

TABLE IV: The distribution of the 200 loop structures according to their length, with the first and last sites in regular secondary structure positions. Two loops with the same length but separated from each other by more than 0.5 Å in RMSD distance are considered different.

Length	5	6	7	8	9
Number	32	116	44	7	1

for developing such a databank by showing that we have a method that works. Consequently we have stopped our search of new loop structures when we reached exactly 200 structures.

In Table V we display how many residues in our entire data set are covered by our 200 loops, when we search for structures using as a criterion the RMSD distance between the structure and a loop. We have performed the search with RMSD cut-off values that range from 0.2 Å to 0.7 Å. The largest value 0.7 Å is selected to slightly exceed the estimate (2). For a cut-off value of 0.6 Å *i.e.*

TABLE V: The coverage of our putative loops in terms of residues, at different RMSD cut-off values. Note that a structure that has between 5 to 9 sites, has a length that is roughly between 20-40 Å.

RMSD cut-off (Å)	Loop sites matched
< 0.2	7.208
< 0.3	31.655
< 0.4	78.561
< 0.5	148.267
< 0.6	245.954
< 0.7	428.387

just below (2) the number of sites in configurations that are covered by our 200 loops already clearly exceeds the total number of sites that are classified as loop sites according to PDB; see Table I. This suggests that we cover all of the loop structures. However, a closer inspection shows that due to overlapping structures the actual coverage is somewhere around 90%. But when the cut-off value reaches 0.7 Å we rarely find any loop structures that remain uncovered. Since we have a very representative data set, this proposes that within the experimental B-factor fluctuation distance accuracy (2), a large majority of *all* loops in PDB, both short and long, are various kind of modular combinations of the 200 *fundamental* loops we have identified.

We now proceed to the second step of our construction. Here we search for parameters in the soliton profile (11), (8) that describe our fundamental 200 loops, so that the RMSD distance between a loop and its soliton is less than 0.5 Å. Since the RMSD distance between any two loop structures in our set of 200 loops is always larger than 0.5 Å, we demand that the pairwise RMSD distance between any two explicit solitons also exceeds 0.5 Å. We estimate the parameters using a Monte Carlo search that

minimizes the RMSD distance between a loop and its soliton. The parameter values are summarized in Figures 2-4:
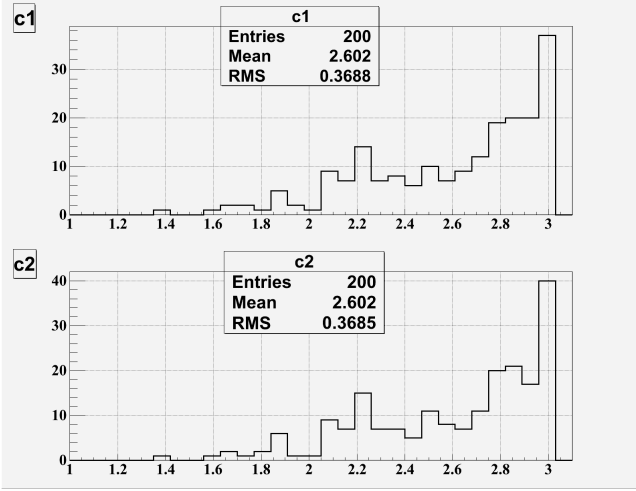

FIG. 2: The distribution of of the parameter value c_1 and c_2 in (5) in the 200 solitons we have constructed. As expected, these two distributions are practically identical.
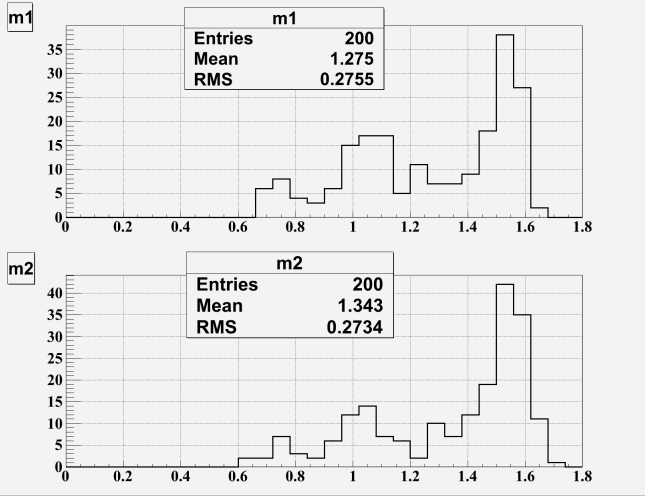

FIG. 3: The distribution of of the parameter values m_1 and m_2 in (5) for the 200 solitons. As in Figure 1, the distributions are highly symmetric, the difference is not statistically meaningful. The α-helices and β-strands (3) are also clearly identifiable in the parameter values.

For each of the 200 loops, we are able to identify parameters so that there is always a soliton profile (11), (8) with explicit parameter values, that describes the loop with RMSD accuracy that is less than 0.5 Å. In fact, as shown in Figure 1 the mean RMSD distance between the original loop configuration and its explicit soliton is a mere 0.14 Å, slightly less than the 0.15 Å estimate for zero point fluctuations in [17]. At this separation distance, it then becomes conceptually meaningless to consider the two structures as different.
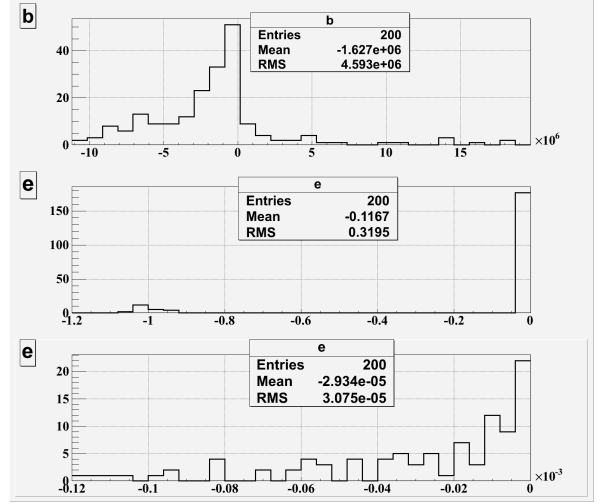

FIG. 4: The distribution of of the parameter values for the torsion angle (6) in our 200 solitons. Observe that the parameter e clusters in two regions, around -1 and below -10^{-4}. Furthermore, the parameter b has very large values, in excess of $\pm 10^6$ and the spread is very large. The fundamental region of the torsion angle θ_i is $[-\pi, \pi]$ and the large values reveal that as a soliton, the loops cover the spheres $(\psi, \theta) \sim \mathbb{S}^2$ several times *i.e.* each of the loop is a multiple soliton configuration. This explains why a very regular soliton such as (5), (6) can model the apparently highly irregular ψ_i and θ_i profiles such as in that we commonly find in PDB.

In Table VI we show how the number of sites that our solitons cover in our full data set depends on the cut-off RMSD distance, for values between 0.2 and 0.7 Å. The results are very similar to those in Table V, there is no practical difference. We also find that when the RMSD cut-off value exceeds (2), the loop structures in our data set that are not fully covered by our 200 explicit solitons become very rare. Consequently we have succeeded in constructing a basis of 200 explicit soliton structures that cover most of the PDB loops, apparently over 90% of them, and with an accuracy that is comparable to the experimental B-factor accuracy.

TABLE VI: The coverage of our explicit soliton configurations in terms of residues, at different RMSD cut-off values.

Cut-off (Å)	Loop sites matched
< 0.2	5.954
< 0.3	28.399
< 0.4	74.037
< 0.5	144.683
< 0.6	245.257
< 0.7	433.737

Finally, we have constructed our 200 explicit solitons by a direct approach, with no attempt for optimization. As a consequence we suspect that the number of explicit solitons can be substantially decreased without compro-

mising the coverage. To show that this is the case we have employed the freedom to choose the integers N_1 and N_2 in (11) independently. These integers are covering numbers, they determine how many times we cover the fundamental domain $\psi \in [-\pi, \pi]$. They have no effect how the parameters m_1 and m_2 determine the asymptotic ψ_i values. Consequently two solitons that differ from each other only by these integers interpolate between regular secondary structures with identical ψ values, and in this sense they can be viewed as different multiple coverings of a single basic soliton with $N_1 = N_2 = 0$. But note that the θ_i values can still be different.

We proceed as follows: We first select a pair of solitons in our library. All the parameters in the first soliton are kept fixed. In the second soliton we also keep all parameters fixed, except that we allow the integers N_1 and N_2 to vary. We then ask whether it is possible to find a new set of integers (N_1, N_2) in the second soliton, so that the RMSD distance between the two solitons becomes less than 0.5 Å. We have found that it is possible to substantially lower the RMSD distance between two solitons. For example, one can find pairs where the initial distance is above 3.5 Å and this becomes lowered to a mere 0.28 Å when we judiciously select the integers (N_1, N_2). In this way we have been able to show that in our set of 200 solitons there are only 57 covering solitons that we fail to bring to within a distance of 0.5 Å from each other. But we suspect that in a carefully constructed and optimized library the number of covering solitons is even much smaller.

IV. EXAMPLES

As an example how the 200 explicit solitons cover our data set at different cut-off values, we show in Figure 5 the typical ψ_i profile of a protein in PDB, we have randomly chosen the one with PDB code 1KZQ. This protein has 289 residues, the experimental resolution is 1.7Å and the observed R-value is 0.2. In the top Figure 5 we use the cut-off value 0.3 Å to locate our solitons. This cut-off value is clearly below the B-factor accuracy of the C_α atoms in 1KZQ, and our 200 solitons cover only around 20 per cent of the loop structures. This coverage is consistent with results in Table VI. When we increase the cut-off value to 0.5 Å (middle Figure 5) most of the loops become covered by solitons, and at 0.7Å there is only one loop with three sites within the loop (*i.e.* a soliton with 5 sites), that does not appear among our 200 solitons. This loop can be modeled by a single soliton and the soliton can be added to our initial unpruned library if so desired, increasing the number of solitons to 201. Alternatively, we could try to describe it as a multiple-covering of one of our 57 solitons. Notice that in addition there are four isolated sites where the deviation exceeds the cut-off value of 0.7 Å. Indeed, it is not too exceptional for proteins that are resolved with this resolution to have individual C_α sites where the experimental accuracy as

measured by the B-factor fluctuation distance exceeds 0.7 Å. These low-resolution C_α carbons commonly become visible in our matching procedure, and this could be used to identify potential problems in data.
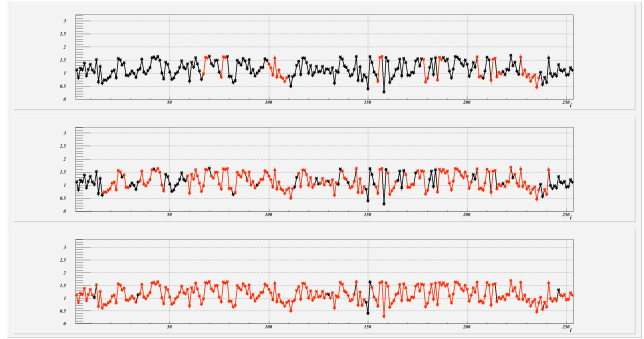

FIG. 5: An example how our 200 explicit solitons cover the protein with PDB code 1KZQ in our data set, in terms of the bond angles ψ_i. We use cut-off values 0.3 Å (top), 0.5 Å (middle) and 0.7 Å (bottom). Red dots and lines correspond to sites and structures that are described by the solitons with the cut-off accuracy or better, while black dots and lines correspond to sites where the local distance exceeds the cut-off value; isolated black dots indicate local fluctuations in B-factors. Three or more consecutive black dots indicate the presence of a loop that is not covered by our 200 solitons. Note that at resolution 0.7 Å (bottom) there is only one such loop.

As a second example we discuss a loop in the protein with PDB code 3DLK. In [17] we showed how to construct a soliton that describes the super-secondary structure that is located between the coordinate sites 398-416 in the A chain of 3DLK, with RMSD accuracy 1.13 Å. The structure describes a loop that connects an α-helix to a β-strand. We now analyze this loop in terms of our library of 200 solitons. In Figure 6a we display the (ψ_i, θ_i) profile around the loop region; We remind that according to (3), (4) the ψ_i is determined by the three coordinate sites i, $i+1$ and $i+2$ while θ_i is determined by the four sites with indices from $i-1$ to $i+2$.

There is a relatively large local fluctuation at the coordinate site i=404, according to the PDB data the B-factor of the C_α atom at this site is 40.0 ($Å^2$) which is clearly above (1). The B-factors at the coordinate sites 403 and 405 are also relatively high, with values 33.5 and 33.5 respectively. But beyond the coordinate site 405, the B-factors are around 25-30 that is the Debye-Waller fluctuation distances are below 0.7 Å for the sites that we have displayed in Figure 6. In Figure 6c the top (red) line shows the fluctuation distances for the coordinate sites 405-414.

In Figure 6b we display the profile of ψ_i, after we have implemented the transformation (6). We clearly identify two soliton profiles (11). Due to the relatively large B-factor at coordinate site 404, we try and take the first soliton to start from the bond angle site 405. The definition of this bond angle is independent of site 404, and
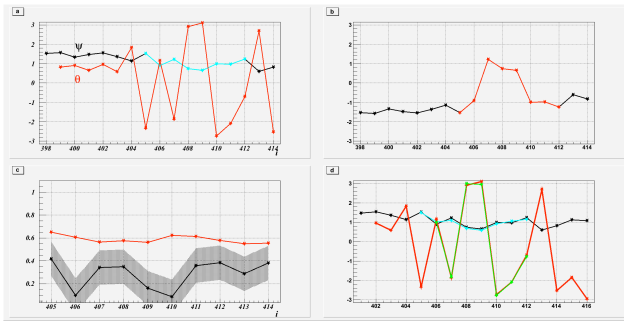
FIG. 6: Figure a) shows the PDB data for the bond and torsion angles for the monomer A in 3DLK, for sites 398-414 Figure b) displays the ψ_i profile, after we have introduced the gauge transformation (6). The two solitons are clearly visible between sites 405-412. In Figure c) we compare the B-factor of the 3DLK (upper line in red) with the distance between its backbone and the two-soliton configuration (lower line with black). The shaded area is the 0.15 Å fluctuation regime around the soliton. In Figure d) we compare the (ψ_i, θ_i) distributions for the PDB data (black and red) and the two-soliton configuration (blue and green).

thus we are optimistic that we do not need to compromise with our ambition to exceed the B-factor accuracy (1) in our loop description. The second soliton ends at bond angle site 412, and the two solitons overlap between the bond angle sites 407 and 409. When we search for similar structures among our 200 solitons, we find two profiles that in combination match the loop. The first soliton covers the coordinate sites 405-410, and the second soliton covers the coordinate sites 409-414. In terms of the bond angles, together they cover the sites 405-412. When we combine these two solitons so that they match each other as accurately as possible at their common coordinate sites 409 and 410, we find a two-soliton configuration that describes the protein loop for residues 405-414 with a RMSD accuracy of 0.31 Å. The (lower) black

line in Figure 6c shows the difference between the PDB structure and the two-soliton structure. This difference is clearly less than the Debye-Waller B-factor distance, at every site. The shaded area describes the zero point fluctuation regime around the solitons. We have followed [17] to estimate that the zero point fluctuations have an amplitude that is no larger than 0.15 Å. Finally, in Figure 6d we compare the ψ_i and θ_i values of the PDB data and the two-soliton configuration. There is essentially no difference.

V. CONCLUSION

Protein loops remain a major challenge both in structure classification and prediction. Loops are commonly viewed as apparently random regions with no regular self-similar structure. Here we have shown that loops are not random at all. Their shape is fully determined and with experimental B-factor accuracy by the dark soliton solution of a generalized discrete nonlinear Schrödinger equation that has only two loop specific parameters. In particular we have found that the number of different parameter sets *i.e.* fundamental loops appears to be no more than 200 and probably it is even smaller than 57 if we allows for multiple coverings. When the fundamental loops together with the helices and strands are at our disposal, the construction of entire folded proteins becomes like a play with Lego bricks. We can build the entire protein from these modular components by simply putting them together, one after another. Moreover, our quantitative approach is firmly grounded on a Physics based energy function. This should enable energetic analyses of protein folding, and energy comparisons between folds and misfolds. We propose that our soliton approach to protein folding can add a powerful component to the existing classification and modeling schemes.

[1] C. Levinthal, Journ. Chim. Phys. et Physico-Chimie Biolog. **65** 44 (1969)

[2] A.G. Murzin, S.E. Brenner, T. Hubbard and C. Chothia, J. Mol. Biol. **247** 536 (1995)

[3] L.H. Greene *et.al* Nucl. Acids Res. **35** D291(2007)

[4] L. Holm , C. Ouzounis, C. Sander, G. Tuparev and G. Vriend Prot. Sci. **1** 1691 (1992)

[5] C. Hadley and D.T. Jones, Structure **7** 1099 (1999)

[6] P.G. Kevrekidis, *The Discrete Nonlinear Schrdinger Equation: Mathematical Analysis, Numerical Computations and Physical Perspectives* (Springer-Verlag, Berlin, 2009)

[7] L.D. Faddeev and L.A. Takhtajan, *Hamiltonian methods in the theory of solitons* (Springer Verlag, Berlin, 1987)

[8] Davydov AS (1977). "Solitons and energy transfer along protein molecules". Journal of Theoretical Biology 66 (2): 379387

[9] A.C. Scott, *Phys. Repts.* **217**, 1 (1992)

[10] H.M. Berman, K. Henrick, H. Nakamura, J.L. Markley , Nucl. Acids Res. (Database issue) 2007, **35** D301-D303

[11] N.Molkenthin, S. Hu, A.J. Niemi Phys. Rev. Lett. **106** 2011, 078102-078105

[12] S. Hu. A. Krokhotin, A.J. Niemi and X. Peng, Phys. Rev. **E 83** 041907 (2011)

[13] G.A.Petsko, D. Ringe Ann. Rev. Biophys. Bioeng. 1984, **13** 331-371

[14] S.Hu, M. Lundgren, A.J. Niemi Phys. Rev. **E83** 2011, 061908-061921

[15] S.Griep, U. Hobohm, Nucl. Acids Res. 2010, (Database issue) **38** D318-D319

[16] M.N.Chernodub, S. Hu, A.J. Niemi Phys. Rev. **E82** 2010, 011916-011920

[17] A.Krokhotin, A.J. Niemi e-print arXiv:1104.2252 [q-bio.BM]